Isı Bilimi ve Tekniği Dergisi, 27, 1, 23-38, 2007
J. of Thermal Science and Technology
©2007 TIBTD Printed in Turkey
ISSN 1300-3615

SOLUTION OF RADIATIVE TRANSFER PROBLEMS IN PARTICIPATING, LINEARLY ANISOTROPICALLY SCATTERING HOLLOW SPHERICAL MEDIUM WITH SK_N METHOD

Mesut TEKKALMAZ* and Zekeriya ALTAÇ**
*Eskişehir Osmangazi University, School of Engineering and Architecture, Metallurgical and Materials Engineering Department, 26480 Batı Meşelik, Eskişehir, tmesut@ogu.edu.tr
**Eskişehir Osmangazi University, School of Engineering and Architecture, Mechanical Engineering Depar-ment,26480 Batı Meşelik, Eskişehir, zaltac@ogu.edu.tr

(Geliş Tarihi: 29. 01. 2007)

Abstract: The Synthetic Kernel (SK_N) approximation is employed to radiative transfer problems of hollow spherical participating and linearly anisotropically scattering medium. The SK_N method relies on approximating the integral transfer kernels by synthetic kernels. The radiative integral transfer equations (RITEs) are then reduced to a set of coupled second-order differential equations. The method is tested against exact solution for various optical geometries, constant and space-dependent scattering albedo variations simulating homogeneous/inhomogeneous medium. It is demonstrated that low order SK_N approximation can be used to solve one dimensional radiative transfer problems of spherical participating medium.
Keywords: Synthetic Kernel Method, Radiative Transfer, Anisotropic Scattering, Spherical Hollow Medium, Participating medium, Concentric sphere.

LİNEER ANİSOTROPİYLE SAÇAN KATILIMCI İÇİÇE KÜRESEL ORTAMDA IŞINIM ISI TRANSFER PROBLEMİNİN SK_N METODU İLE ÇÖZÜMÜ

Özet: Sentetik Kernel metodu, soğuran, yayan ve lineer anizotropiyle saçan içiçe küresel ortamların ısıl ışınım problemlerine uygulanmıştır. Metot, ışınım integral taşınım kernellerine sentetik kerneller ile yaklaşımda bulunmak suretiyle, bir takım-diferansiyel denklem sistemine indirgenmesi esasına dayanır. Metot, çeşitli optik geometriler, homojen ve homojen olmayan ortamların simülasyonunda, sabit ve uzay-bağımlı saçılma albedo değişimlerine karşın ışınım integral denkleminin gerçek çözümüyle karşılaştırılmıştır. Düşük mertebeli SK_N yaklaşımın bir boyutlu küresel katılımcı ortam ışınım taşınımı problemlerinin çözümünde kullanılabileceği gösterilmiştir.
Anahtar Kelimeler: Sentetik Kernel Metodu, Işınım Isı transferi, Anizotropik saçılma, İçiçe küresel ortam, Katılımcı ortam, İçiçe küre.

NOMENCLATURE

$E_n(x)$	n^{th} order exponential integral function
$G(\tau)$	dimensionless incident radiation $(= 2\pi\int_{-1}^{1} I(\tau,\mu)d\mu)$
$G_n(\tau)$	expression defined by Eq. (16)
$I(\tau,\mu)$	dimensionless radiative intensity $(= i(\tau,\mu)/(n^2\sigma T_{ref}^4/\pi))$
K_1^G, K_2^G	transfer kernels of incident energy given by Eqs. (5) and (6)
K_1^q, K_2^q	transfer kernels of heat flux given by Eqs. (7) and (8)
$S_0(\tau)$	dimensionless isotropic source function given by Eqs. (5) $(= s_0/(n^2\sigma T_{ref}^4/\pi))$
$S_1(\tau)$	dimensionless anisotropic source function given by Eqs. (6) $(= s_1/(n^2\sigma T_{ref}^4/\pi))$
$T(\tau)$	temperature
a_1	coefficient of linear anisotropy
$f_1(\tau), f_2(\tau)$	boundary terms defined by Eqs. (9) and (10)
$q(\tau)$	dimensionless radiative heat flux $(= 2\pi\int_{-1}^{1} I(\tau,\mu)\mu d\mu)$
$q_n(\tau)$	expression defined by Eq. (17)
w_n	Gauss quadrature weights
Greek symbols	
Γ	hemispherical transmissivity
$\Omega_0(\tau)$	scattering albedo ($\sigma(\tau)/\beta$)
β	extinction coefficient
$\kappa(\tau)$	absorption coefficient
μ_n	Gauss quadrature abscissas

$\theta(\tau)$	dimensionless temperature ($=T(\tau)/T_{ref}$)
ρ	hemispherical reflectivity
$\sigma(\tau)$	scattering coefficient
τ	dimensionless optical variable (=rβ)
Subscripts	
n	n^{th} component of the SK_N equations
ref	reference
w	wall

INTRODUCTION

Radiative transfer in spherical participating medium has numerous applications in insulation and combustion systems, thermal manufacturing processes, particulate solar collectors, nuclear engineering, astrophysics, and environmental and space sciences such as prediction of the effect of dust and participating gases on the global environment.

The exact formulation of the radiative transfer equation (RTE) is the radiative integral transfer equation (RITE). The exact integral equations for any geometry and/or arbitrary boundary condition cannot be generalized due to the difficulty in finding the geometry-dependent integral transfer kernels which require analytical derivations. The integral transfer kernels are mathematically singular in nature, and the numerical solution of the RITE also requires special techniques to avoid or remove singularities. Therefore, a number of numerical methods have been developed over last few decades to solve thermal radiative transfer problems in participating medium. Monte-Carlo, zonal method, spherical harmonics (P_N), discrete ordinate method (DOM), differential and modified differential approximations, collocation and variational methods have been proposed and used for various geometries, including spherical medium. However, every one of the methods mentioned also has its own limitations in certain cases and/or geometries.

Radiative transfer in a participating homogeneous or inhomogeneous solid spherically symmetric medium with isotropic or linearly anisotropic scattering has been the subject of numerous studies (Traugot, 1969; Thynel and Özısık, 1985a; Thynel and Özısık, 1985b; Thynel and Özısık, 1986; El-Wakil et al., 1988; Thynell, 1989; Wilson and Nanda, 1990; El-Wakil et al., 1991; Sghaier, et al., 2000). The radiative transfer in paricipating hollow or concentric spherical medium has also been studied with various methods (Ryhming, 1966; Viskanta and Crosbie, 1967; Olfe, 1968; Crosbie and Khalil, 1972; Tong and Swathit, 1987; Tsai, et al., 1989; Jia, et al., 1991; Li and Tong, 1990; Altaç and Tekkalmaz, 2004; Trabelsi, et al., 2005) such as discrete ordinates method (DOM), spherical harmonics, variational and collocation. These methods in principle require the solution of either the radiative transfer equation (RTE) or the radiative integral transfer equation (RITE) for intensity, incident energy and radiative heat flux. The discrete ordinates method (DOM or S_N method) had first found applications in neutron transport. In the last two decades, the DOM has evolved and quickly became the dominant mean of obtaining numerical solutions in radiative transfer, and it is considered to be potential and a very promising tool for treating thermal radiation problems. Although the method yields results of sufficient accuracy for most engineering problems; the DOM is also plagued with so called "ray effect" in rectangular and curvilinear geometries (Lewis and Miller, 1984). The main cause of ray effect is the angular discretization. As a remedy, one could simply increase the number of directions; however, the ray effect still persists (Lewis and Miller, 1984). Comparisons of the RTE solutions for rectangular geometries with the exact, P_1, S_4, S_8, S_{16}, SK_1 and SK_2 methods confirm that the SK_N solutions are free of ray effect while distinct ray effect oscillations even in S_{16} solutions are observed (Altaç and Tekkalmaz, 2003). Additionally, in curvilinear geometries a great deal of difficulties has to be dealt with due to the streaming term, directional derivative, of RTE.

The incident energy and the radiative heat flux in the RITEs contain only spatial variables since the angular dependence is completely eliminated due to integration of intensity over the solid angle. On the other hand, one of the major disadvantages of treating the RITEs is that the numerical solution of the RITEs results in dense matrices. In one dimensional geometries, this may not be a great concern; however, particularly, in multidimensional geometries this consequence may require restrictions on the computational memory and execution time. The second major disadvantage of dealing with RITEs is the integral transfer kernels for a specific geometry must be derived analytically, and for complicated geometries the derivation of the transfer kernels is a difficult task, not to mention the singularities that should be tackled analytically or computationally.

The Synthetic Kernel (SK_N) method deals with the RITEs, and it consists of an approximation, in the form of exponentials, to the RITE kernels similar to the exponential kernel approximation. Then, the RITEs, in multidimensional geometries, can be cast as a set of coupled elliptic second-order partial differential equations, or ordinary differential equations in one dimensional geometries. Thus, one does not have to deal with the singularity removal of the transfer kernels. The method was first employed to neutron transport problems of homogeneous and inhomogeneous medium (Altaç and Spinrad, 1990; Spinrad and Altaç, 1990), the SK_N solutions—which consisted of benchmark problems with stepwise changing medium properties—agreed remarkably well with those of the spherical harmonics, DOM and Monte-Carlo. Recently, the method was applied to two-dimensional thermal radiative transfer problems (Altaç, 1997; Altaç and Tekkalmaz, 2002). The foregoing studies used the half-range Gauss quadrature set to obtain the approximate synthetic kernels. The method was also extended to linearly anisotropically scattering participating homogeneous and inhomogeneous plane-parallel medium (Altaç, 2002a; Altaç, 2002b), and the SK_N solutions of the benchmark problems compared extremely well those of high order spherical harmonics P_N, DOM and RITE. The method was later applied to an absorbing, emitting, and isotropically scattering homogeneous and inhomogeneous solid spherical medium (Altaç and Tekkalmaz, 2003). The performance of the SK_N method was explored in comparison to the test problems with the exact and S_8 solutions. Most recently, the SK_N method was employed to homogeneous and inhomogeneous one- and two-dimensional (*r*-z) geometries (Döner and Altaç, 2006a; Döner and Altaç, 2006b; Döner and Altaç, 2006c). These studies show that the method can be used to obtain very accurate solutions with less computational efforts.

In this paper, the SK_N method is extended to radiative transfer in linearly anisotropically scattering participating hollow sphere medium. The geometry and the benchmark problem is unique in that it has an internal boundary unlike other foregoing problems tackled so far. The performance of the method with an internal boundary is investigated by comparing the SK_N solutions quantitatively and qualitatively with exact RITE solutions.

DERIVATION OF THE RITE FOR SPHERICAL SHELL MEDIUM

For general coordinate systems, the dimensionless form of the RITE for homogeneous absorbing, emitting and linearly anisotropically scattering medium is given in Altaç (2003). The derivations of the RITEs for spherical media is carried out using the general forms—Eqs. (12) and (13) of Altaç (2003). The geometry and the coordinate system is shown in Figure 1.

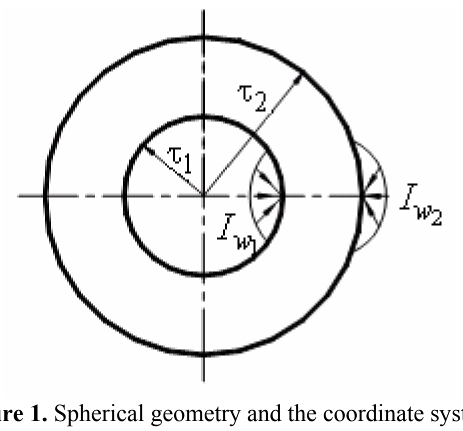

Figure 1. Spherical geometry and the coordinate system.

To obtain the RITEs for one-dimensional spherical medium, we perform the integrations of Eqs. (12) and (13) over the azimuthal and polar angles. Then the monochromatic dimensionless RITEs for one-dimensional hollow spherical medium can be written as, for the incident energy,

$$G(\tau) = f_1(\tau) + \int_{\tau'=\tau_1}^{\tau_2} K_1^G(\tau,\tau') S_0(\tau') d\tau' + a_1 \int_{\tau'=\tau_1}^{\tau_2} K_2^G(\tau,\tau') S_1(\tau') d\tau' \quad (1)$$

and for the net radiative heat flux

$$q(\tau) = f_2(\tau) + \int_{\tau'=\tau_1}^{\tau_2} K_1^q(\tau,\tau') S_0(\tau') d\tau' + a_1 \int_{\tau'=\tau_1}^{\tau_2} K_2^q(\tau,\tau') S_1(\tau') d\tau' \quad (2)$$

where $S_0(\tau)$ and $S_1(\tau)$ are the isotropic and anisotropic source functions which are defined as

$$S_0(\tau) = 4\pi[1-\Omega_0(\tau)]\theta^4(\tau) + \Omega_0(\tau)G(\tau) \quad (3)$$

and

$$S_1(\tau) = \Omega_0(\tau) q(\tau) \quad (4)$$

where $\theta(\tau)=T(\tau)/T_{ref}$ is the dimensionless temperature, Ω_0 is the space-dependent scattering albedo given by $\Omega_0=\sigma(\tau)/\beta$ and $\beta=\sigma(\tau)+\kappa(\tau)$ which is the extinction coefficient, $\sigma(\tau)$ and $\kappa(\tau)$ are the space-dependent scattering and absorption coefficients, respectively, and $[1-\Omega_0(\tau)]\theta^4(\tau)$ is the dimensionless blackbody radiation intensity.

The integral transfer kernels of incident energy are, expressed with superscript *G*, can be written as follows:

$$K_1^G(\tau,\tau') = \frac{\tau'}{2\tau}\left\{E_1(|\tau-\tau'|) - E_1(\lambda(\tau,\tau'))\right\} \quad (5)$$

and

$$K_2^G(\tau,\tau') = \frac{1}{2\tau}\left\{\begin{array}{l} \tau'\,\mathrm{sgn}(\tau-\tau')E_2(|\tau-\tau'|) \\ +\eta(\tau',\tau_1)E_2(\lambda(\tau,\tau')) \\ -E_3(|\tau-\tau'|) + E_3(\lambda(\tau,\tau')) \end{array}\right\} \quad (6)$$

where $\lambda(\tau,\tau') = \sqrt{\tau^2-\tau_1^2} + \sqrt{\tau'^2-\tau_1^2}$ and $\eta(\tau,\tau') = \sqrt{\tau^2-\tau'^2}$ definitions have been adapted here to save space and to present equations in a coherent fashion.

On the other hand, transfer kernels of net radiative heat flux, expressed with superscript *q*, are written as

$$K_1^q(\tau,\tau') = \frac{\tau'}{2\tau^2}\left\{\begin{array}{l} \tau\,\mathrm{sgn}(\tau-\tau')E_2(|\tau-\tau'|) \\ -\eta(\tau,\tau_1)E_2(\lambda(\tau,\tau')) \\ +E_3(|\tau-\tau'|) - E_3(\lambda(\tau,\tau')) \end{array}\right\} \quad (7)$$

and

$$K_2^q(\tau,\tau') = \frac{1}{2\tau^2}\left\{\begin{array}{l} \tau\tau' E_3(|\tau-\tau'|) \\ +\eta(\tau,\tau_1)\eta(\tau',\tau_1)E_3(\lambda(\tau,\tau')) \\ +\lambda(\tau,\tau')E_4(\lambda(\tau,\tau')) \\ -|\tau-\tau'|E_4(|\tau-\tau'|) \\ -E_5(|\tau-\tau'|) + E_5(\lambda(\tau,\tau')) \end{array}\right\} \quad (8)$$

where sgn(τ-τ′) is the sign function.

Incident diffuse radiation from the inner and outer shell surfaces are expressed as

$$f_1(\tau)=\frac{I_{w1}}{2\tau}\begin{Bmatrix}\tau_1 E_2(\tau-\tau_1)+E_3(\eta(\tau,\tau_1))\\ -E_3(\tau-\tau_1)\end{Bmatrix}+\frac{I_{w2}}{2\tau}\begin{Bmatrix}\tau_2 E_2(\tau_2-\tau)\\ -\eta(\tau_2,\tau_1)E_2(\lambda(\tau_2,\tau))\\ +E_3(\tau_2-\tau)-E_3(\lambda(\tau_2,\tau))\end{Bmatrix} \tag{9}$$

and

$$f_2(\tau)=\frac{I_{w1}}{2\tau^2}\begin{Bmatrix}\tau\tau_1 E_3(\tau-\tau_1)\\ -(\tau-\tau_1)E_4(\tau-\tau_1)\\ +\eta(\tau,\tau_1)E_4(\eta(\tau,\tau_1))\\ -E_5(\tau-\tau_1)+E_5(\eta(\tau,\tau_1))\end{Bmatrix}+\frac{I_{w2}}{2\tau^2}\begin{Bmatrix}-\tau\tau_2 E_3(\tau_2-\tau)\\ -\eta(\tau_2,\tau_1)\eta(\tau,\tau_1)E_3(\lambda(\tau_2,\tau))\\ -\lambda(\tau_2,\tau)E_4(\lambda(\tau_2,\tau))\\ +(\tau_2-\tau)E_4(\tau_2-\tau)\\ +E_5(\tau_2-\tau)-E_5(\lambda(\tau_2,\tau))\end{Bmatrix} \tag{10}$$

where I_{w1} and I_{w2} are the incident diffuse radiation intensities of inner and outer shells, respectively.

DERIVATION OF THE SK$_N$ EQUATIONS

The exact radiative transfer kernels are replaced with a sum of exponentials. The rational behind the synthetic kernel approximation of the RITEs kernels and quadrature selection is given in detail in Altaç (2002a). For the *m*th order exponential integral functions, we use the the following finite sum obtained by the *N*-point Gaussian integration over $\mu\in(0,1)$ interval:

$$E_m(x)=\int_0^1 \mu^{m-2}e^{-x/\mu}d\mu \cong \sum_{n=1}^{N} w_n\mu_n^{m-2}e^{-x/\mu_n} \quad \text{for } m=1,\cdots,5 \tag{11}$$

where w_n and μ_n's are quadrature weights and abscissas over the prescribed interval. These quadratures are tabulated for various *N* values in Abramowitz and Stegun (1964). Using the same form of the exponential sum for $E_m(x)$, one can obtain various quadrature sets to improve the accuracy of the synthetic kernels (Altaç, 2002a).

To start the derivation of the SK_N equations, we substitute the approximations by Eq. (11) into the exponential integral functions in Eq. (1) and (2), and we define *n*th component of the kernels as

$$\tilde{K}_{1,n}^{G}(\tau,\tau')=\frac{\tau'}{2\tau\mu_n}\begin{Bmatrix}\exp(-|\tau-\tau'|/\mu_n)\\ -\exp(-\lambda(\tau,\tau')/\mu_n)\end{Bmatrix} \tag{12}$$

$$\tilde{K}_{2,n}^{G}(\tau,\tau')=\frac{1}{2\tau}\begin{Bmatrix}\tau'\mathrm{sgn}(\tau-\tau')\exp(-|\tau-\tau'|/\mu_n)\\ +\eta(\tau',\tau_1)\exp(-\lambda(\tau,\tau')/\mu_n)\\ -\mu_n\exp(-|\tau-\tau'|/\mu_n)\\ +\mu_n\exp(-\lambda(\tau,\tau')/\mu_n)\end{Bmatrix} \tag{13}$$

$$\tilde{K}_{1,n}^{q}(\tau,\tau')=\frac{\tau'}{2\tau^2}\begin{Bmatrix}\tau\ \mathrm{sgn}(\tau-\tau')\exp(-|\tau-\tau'|/\mu_n)\\ -\eta(\tau,\tau_1)\exp(-\lambda(\tau,\tau')/\mu_n)\\ +\mu_n\exp(-|\tau-\tau'|/\mu_n)\\ -\mu_n\exp(-\lambda(\tau,\tau')/\mu_n)\end{Bmatrix} \tag{14}$$

and

$$\tilde{K}_{2,n}^{q}(\tau,\tau')=\frac{1}{2\tau^2}\begin{Bmatrix}\tau\tau'\mu_n\exp(-|\tau-\tau'|/\mu_n)\\ +\eta(\tau,\tau_1)\eta(\tau',\tau_1)\mu_n\exp(-\lambda(\tau,\tau')/\mu_n)\\ +\mu_n^2\lambda(\tau,\tau')\exp(-\lambda(\tau,\tau')/\mu_n)\\ -\mu_n^2|\tau-\tau'|\exp(-|\tau-\tau'|/\mu_n)\\ -\mu_n^3\exp(-|\tau-\tau'|/\mu_n)\\ +\mu_n^3\exp(-\lambda(\tau,\tau')/\mu_n)\end{Bmatrix} \tag{15}$$

We also define the following quantities

$$G_n(\tau)=\int_{\tau'=\tau_1}^{\tau_2}\tilde{K}_{1,n}^{G}(\tau,\tau')S_0(\tau')d\tau'+a_1\int_{\tau'=\tau_1}^{\tau_2}\tilde{K}_{2,n}^{G}(\tau,\tau')S_1(\tau')d\tau' \tag{16}$$

and

$$q_n(\tau)=\int_{\tau'=\tau_1}^{\tau_2}\tilde{K}_{1,n}^{q}(\tau,\tau')S_0(\tau')d\tau'+a_1\int_{\tau'=\tau_1}^{\tau_2}\tilde{K}_{2,n}^{q}(\tau,\tau')S_1(\tau')d\tau' \tag{17}$$

It is important to note that Eqs. (16) and (17) do not have any physical meanings. Using (16) and (17), Eq. (1) and (2) can be rewritten as

$$G(\tau)=f_1(\tau)+\sum_{n=1}^{N}w_nG_n(\tau) \tag{18}$$

and

$$q(\tau)=f_2(\tau)+\sum_{n=1}^{N}w_nq_n(\tau) \tag{19}$$

At this stage, to get quantities of physical interest, namely $G(\tau)$ and $q(\tau)$, we need to find solutions for Eqs. (16) and (17). Here, the derivation of SK_N equations for a solid sphere is given by setting $\tau_1=0$ in Eqs. (16) and (17), then appropriate boundary conditions for hollow medium is imposed. Under foregoing assumptions, it can be shown that $G_n(\tau)$ and $q_n(\tau)$ satisfy the following coupled first-order differential equations by taking the derivatives of Eqs. (16) and (17) with respect to τ:

$$q_n(\tau) = -\mu_n^2 \frac{dG_n(\tau)}{d\tau} + a_1 \, \mu_n^2 \, S_1(\tau) \tag{20}$$

and

$$\frac{d}{d\tau}\left[\tau^2 q_n(\tau)\right] = -\tau^2 G_n(\tau) + \tau^2 S_0(\tau) \tag{21}$$

When taking the derivative of the RHS of Eq. (20), we have to deal with the following term:

$$\frac{d}{d\tau}\left[\Omega_0(\tau)\tau^2 q(\tau)\right] = \frac{d\Omega_0}{d\tau}\tau^2 q(\tau) + \Omega_0(\tau)\frac{d}{d\tau}\left[\tau^2 q(\tau)\right] \tag{22}$$

We can use the energy balance given by Eq. (23) on the second term of Eq. (22).

$$\text{div}\,\mathbf{q} = \frac{d\left(\tau^2 q(\tau)\right)}{\tau^2 d\tau} = \left(1-\Omega_0(\tau)\right)\left[4\pi\theta^4(\tau) - G(\tau)\right] \tag{23}$$

We use Eqs. (3), (4) and (23), and rearrange the remaining expressions to eliminate $q_n(\tau)$ from Eqs. (20) and (21). We then finally obtain—so called—the SK_N equations (for n=1,2,…N) as follows:

$$\begin{aligned} -\mu_n^2 \frac{1}{\tau^2}\frac{d}{d\tau}\left[\tau^2 \frac{dG_n}{d\tau}\right] + G_n(\tau) &= 4\pi\left[1-\Omega_0(\tau)\right]\left[1 - a_1\,\mu_n^2\,\Omega_0(\tau)\right]\theta^4(\tau) \\ &+ \Omega_0(\tau)\left[1 + a_1\,\mu_n^2\,\left[1-\Omega_0(\tau)\right]\right]G(\tau) \\ &- a_1\,\mu_n^2\,q(\tau)\frac{d\Omega_0}{d\tau} \end{aligned} \tag{24}$$

Thermal radiation boundary conditions for hollow spherical medium are already included in surface integrals through force functions $f_1(\tau)$ and $f_2(\tau)$ —Eqs. (9) and (10). However, we need a set of alternative boundary conditions of mathematical in nature to be able solve the SK_N equations. A couple of boundary conditions can be obtained by simply evaluating the limits of $G_n(\tau)$ and $q_n(\tau)$ for $\tau\to\tau_1$ and $\tau\to\tau_2$ surfaces. Having done that two boundary conditions yield for the inner shell

$$\frac{dG_n(\tau_1)}{d\tau} + \left(\frac{1}{\tau_1} - \frac{1}{\mu_n}\right)G_n(\tau_1) = a_1\Omega_0(\tau_1)q(\tau_1) \tag{25}$$

and for the outer shell

$$\frac{dG_n(\tau_2)}{d\tau} + \left(\frac{1}{\tau_2} + \frac{1}{\mu_n}\right)G_n(\tau_2) = a_1\Omega_0(\tau_2)q(\tau_2) \tag{26}$$

These boundary conditions are to be used regardless of the physical boundary conditions imposed on the inner and/or outer shells. However, for solid spherical geometry, the boundary condition at the center becomes $dG_n(\tau_1)/d\tau=0$ (Altaç and Tekkalmaz, 2003).

To find an SK_N expression for the net radiative heat flux, we substitute $q_n(\tau)$ from Eq. (20) in Eq. (21), along with the use of Eqs. (3) and (4), solving it for $q_n(\tau)$ we obtain:

$$q(\tau) = \left(f_2(\tau) - \sum_{n=1}^{N} w_n\mu_n^2 \frac{dG_n}{d\tau}\right) \Bigg/ \left(1 - a_1\Omega_0(\tau)\sum_{n=1}^{N} w_n\mu_n^2\right) \tag{27}$$

Equation (27) allows us to compute the net radiative heat flux with only $G_n(\tau)$ information. However, one can obtain net heat flux by integrating Eq. (21) over the control volume starting from the inner shell towards the outer shell.

RESULTS AND DISCUSSION

The following benchmark problems have been considered for the quantitative and qualitative comparisons of the SK_N method's performance with the exact RITE solutions.

Benchmark Problem 1 (BMP-1). The problem of radiative transfer in a hollow spherical participating medium with a constant scattering albedo (homogeneous medium) and transparent outer shell boundary is considered. The main source in the medium is due to the externally isotropic unit incidence of radiation at the outer shell of the sphere $\tau=\tau_2$; that is, $I_{w2}=1$. The linearly anisotropic scattering medium is cold. The hemispherical reflectivity and transmissivity of the outer shell which are defined as $\rho=q^+(\tau_2)/q^-(\tau_2)$ and $\Gamma=q^-(\tau_1)/q^-(\tau_2)$, respectively, are computed for hollow spherical medium of $\tau_1=1.0$, $\tau_2=2.0$ (Case A), $\tau_1=1.0$, $\tau_2=4.0$ (Case B), and $\tau_1=4.0$, $\tau_2=5.0$ (Case C). These parameters are computed for constant scattering albedo values ranging from $\Omega_0=0.1$ to $\Omega_0=0.9$, and for coefficient of linear anisotropy values of $a_1=-1$ (back scattering), $a_1=0$ (isotropic scattering) and $a_1=1$ (forward scattering).

Benchmark Problem 2 (BMP-2). The medium is inhomogeneous *via* the space-dependent scattering albedo. As in BMP-1, the medium is also cold and is subject to the externally isotropic unit incidence of radiation on the outer shell ($I_{w2}=1$) with the same optical dimensions. For the three hollow spherical geometries (Cases A, B and C), the following space-dependent scattering albedos are considered: linear albedo variations of $\Omega_0(\tau)=0.25+\tau/3F_1$ and $\Omega_0(\tau)=0.75-\tau/3F_1$ and quadratic albedo variations of $\Omega_0(\tau)=0.4-4\tau/15F_1+\tau^2/2F_2$ and $\Omega_0(\tau)=1-16\tau/15F_1+\tau^2/2F_2$ where $F_n=(\tau_2^{n+3}-\tau_1^{n+3})/(\tau_2^3-\tau_1^3)$. Similarly the effect of the coefficient of linear anisotropy values of $a_1=-1$ (back scattering), $a_1=0$ (isotropic scattering) and $a_1=1$ (forward scattering) on the numerical solutions is investigated. The space-dependent albedos are chosen such that the scattering property of the medium increases from the inner to the outer shell or *vice versa*. The average value of $\Omega_0(\tau)$ over the medium is equal to 0.5 in all the cases.

Numerical Solution Techniques

In this study, $\tau_1\leq\tau\leq\tau_2$ interval is equally divided into N grid elements in numerical solutions of both the RITE and the SK_N equations. The RITEs are solved using *subtraction of singularity* technique (Altaç, 2002a; Altaç, 2002b; Altaç and Tekkalmaz, 2003; Döner and Altaç, 2006). The numerical integrations are carried out using Simpson's rule, which has a fourth order truncation error, while the integrals which possess singular points at $\tau=\tau'$ are evaluated analytically. The resulting system of linear equations is solved using Gauss elimination technique. The SK_N equations, however, were solved iteratively as described in Altaç (2002a). The convergence criterion based on relative errors for all methods was $\zeta<10^{-6}$. The direct numerical solution techniques can very well be implemented as discussed in Altaç (2002a).

Several cases of grid configurations, ranging from 200 to 800, were considered to ensure grid independent solutions. In Table 1, the transmissivity and reflectivity values for outer shell, along with the cpu-time for 800 grids, using the exact RITE, DOM S_8, S_{12}, S_{16} and SK_N solutions up to the third order, are listed for Ω_0=0.7 of Case A, B and C of BMP-1. The DOM solutions were obtained by the quadratures provided by Lee (1962). It is observed that the RITE solutions converge five significant figure accuracy with 400 grids while the SK_N solutions required 800 grids since a second order finite difference formulations were used in discretization of the SK_N equations.

For Case A and 800 intervals, absolute errors of the reflectivity and transmissivity with respect to the exact solution yield, respectively, 1.1% and 0.61% for S_8, –0.75% and 0.75% for S_{12}, –0.57% and 0.36% for S_{16}. On the other hand, these errors are 1.3% and –0.24% for SK_1, -0.63% and –1.23% for SK_2 and –0.64% and –1.11% for SK_3 approximations, respectively. The order of magnitude of the errors for DOM and SK_N methods are almost the same. The errors in transmissivity are slightly higher than those of the DOM. The cpu-times for the exact, DOM S_8, S_{12} and S_{16} are 17.5313, 0.0469, 0.0625 and 0.0938 seconds, respectively, while these values for SK_1, SK_2 and SK_3 are 0.2031, 0.4219 and 0.5313 seconds.

For Case B and 800 grid intervals, the reflectivity and transmissivity errors yield, respectively, –1.16% and

Table 1. Grid sensitivity and cpu-time analysis for Ω_0=0.7 of Cases A, B and C of BMP-1.

	N=200		*N*=400		*N*=800		
Case A	ρ	Γ	ρ	Γ	ρ	Γ	cpu-time (s)
Exact	0.46060	0.53670	0.46060	0.53669	0.46060	0.53669	17.531
S_8	0.47159	0.53060	0.47159	0.53060	0.47159	0.53060	0.047
S_{12}	0.46812	0.53207	0.46812	0.53207	0.46812	0.53207	0.062
S_{16}	0.46628	0.53313	0.46628	0.53313	0.46628	0.53313	0.093
SK_1	0.44758	0.53912	0.44757	0.53911	0.44757	0.53911	0.203
SK_2	0.46686	0.54899	0.46686	0.54898	0.46686	0.54898	0.422
SK_3	0.46696	0.54785	0.46696	0.54785	0.46696	0.54784	0.531
Case B							
Exact	0.37219	0.16063	0.37217	0.16063	0.37216	0.16063	18.812
S_8	0.38372	0.15871	0.38372	0.15871	0.38372	0.15871	0.047
S_{12}	0.38010	0.15886	0.38010	0.15886	0.38010	0.15886	0.109
S_{16}	0.37820	0.15913	0.37820	0.15913	0.37820	0.15913	0.156
SK_1	0.36168	0.16925	0.36164	0.16923	0.36163	0.16922	0.375
SK_2	0.37221	0.16677	0.37217	0.16674	0.37216	0.16674	0.672
SK_3	0.37269	0.16764	0.37265	0.16762	0.37264	0.16761	0.875
Case C							
Exact	0.29797	0.44162	0.29797	0.44162	0.29797	0.44162	17.766
S_8	0.30982	0.43563	0.30982	0.43563	0.30982	0.43563	0.047
S_{12}	0.30607	0.43751	0.30607	0.43751	0.30607	0.43751	0.062
S_{16}	0.30414	0.43846	0.30414	0.43846	0.30414	0.43846	0.109
SK_1	0.28387	0.43581	0.28387	0.43580	0.28387	0.43580	0.187
SK_2	0.29868	0.44375	0.29867	0.44375	0.29867	0.44375	0.359
SK_3	0.29873	0.44296	0.29873	0.44296	0.29873	0.44296	0.468

0.19% for S_8, –0.79% and 0.18% for S_{12}, –0.6% and 0.15% for S_{16} while these errors turn out to be 1.05% and –0.86% for SK_1, 0.0% and –0.611% for SK_2 and –0.05% and –0.69% for SK_3, respectively. In this case, the reflectivity values obtained with SK_2 and SK_3 are better than those of the DOM solutions; on the other hand, the transmissivity values obtained with the DOM are about 0.5% better those of the SK_N approximations. The cpu-times for the exact, DOM S_8, S_{12} and S_{16} are 18.8125, 0.0469, 0.1094 and 0.1563 seconds, respectively. For SK_1, SK_2 and SK_3, the cpu-times are 0.375, 0.6719 and 0.875 seconds. Finally, for Case C and 800 grid intervals, the reflectivity and transmissivity result in absolute errors of –1.18% and 0.6% for S_8, –0.81% and 0.41% for S_{12}, –0.62% and 0.32% for S_{16} respectively. The absolute errors become 1.41% and 0.58% for SK_1, –0.07% and –0.21% for SK_2 and –0.08% and –0.13% for SK_3, respectively. In this case, the accuracy of SK_2 and SK_3 approximations are better than the DOM yielding about 0.7% and 0.2% less errors for the reflectivity and transmissivity, respectively. The cpu-times are for the exact, DOM S_8, S_{12} and S_{16} are 17.7656, 0.0469, 0.0625 and 0.1094 seconds, respectively. For SK_1, SK_2 and SK_3, the cpu-times are 0.1875, 0.3593 and 0.46885 seconds.

The cpu-times of the DOM and the SK_N methods are significantly lower than those of the exact RITE solutions. The cpu time is clearly affected by the initial guesses made for the quantities involved. In this study, the initial guesses for all quantities were taken to be zero. For radiation, convection and/or conduction combined heat transfer problems, the exact solution strategy becomes inapropriate because of its excessive computation time while the computation times of the DOM and SK_N methods are competitive. On the other hand, it is worth mentioning that the DOM quadratures for the plane parallel and spherical geometries requires only N directions whereas the number of discrete directions in one dimensional cylindrical geometry and multi-dimensional geometries are N(N+2) which results in significant increase in the cpu-time for high order DOM solutions.

Homogeneous Medium

The hemispherical reflectivity and transmissivities for Cases A, B and C were computed with the exact RITEs and the SK_N method are comparatively presented in Table 2. In all the cases, for mostly absorbing medium (Ω_0<0.2), the SK_1 approximation yields both reflectivity and transmissivity values of at least three significant digit accurate values (absolute errors of less than 0.02%) with those of the exact RITE solutions. As expected, the SK_2 solutions exhibit improvement over SK_1 solutions yielding 5 to 6 significant accurate values (absolute errors of less than 0.007%). The highest errors are observed in Ω_0=0.9 cases. For Case A and for Ω_0=0.9, the absolute errors for the reflectivity and transmissivity with SK_1 approximation results in 1.421%, –0.177%; 1.303%, –0.242% and 1.126%, –0.137%, respectively, for backward, isotropic and forward scattering medium. On the other hand, these errors for SK_2 approximation yield -0.369%, –1.415%; –0.629%, –1.229% and –1.007%, –0.707%, respectively, for backward, isotropic and forward scattering medium. For Case B and for Ω_0=0.9, the absolute errors for the reflectivity and transmissivity with SK_2 approximation, for backward, isotropic and forward scattering medium, are –0.216%, –3.552%; –0.375%, –3.096% and –0.647%, –1.752%, respectively while, for Case C, these errors become –0.205%, –6.16%; –0.296%, –0.593% and –0.439%, –0.527%. The magnitude of the SK_N errors are about the same order with high order DOM errors presented in Table 1. The absolute errors medium with scattering albedos of less than 0.9 are much less.

The incident radiation and the net radiative heat flux profiles for the whole solution domain are obtained with the exact RITE, SK_1, SK_2 and SK_3 for Case A (BMP-1 and Ω_0=0.5) and qualitatively presented for isotropic, forward and backward scattering medium in Figure 2. The incident radiation profiles of the SK_N solutions exhibit very good agreement with those of RITE in all scattering cases. While the incident energy profiles of the SK_1 approximation slightly deviate from the exact solutions, the deviations in the SK_2 and SK_3 approximations are much smaller in magnitude. On the other hand, the net radiative heat flux profiles show deviations of larger magnitude near the inner shell with the SK_2 and SK_3 solutions. However, the deviations from the SK_1 solutions are smaller.

In Figure 3, the exact RITE and the SK_N solutions of the net radiative heat flux profiles of Case B and C, for Ω_0=0.5 and for isotropic, forward and backward anisotropic scattering medium are depicted. In both cases, the SK_N solutions are in excellent agreement with those of exact RITE, with only exception that, at the inner shell surface, the SK_1 approximation exhibits slight deviations in isotropic and forward scattering medium of Case B (Figs. 3(b) and (c)). This phenomenon is also observed in Case A. Both cases are geometries of small inner optical radius. As it is obvious from Case C (τ_1=4), the deviations throughout the medium is diminished. This trend was observed in other cases with small inner shell radius (τ_1<1).

As the scattering albedo increases, the reflectivity and transmissivity values yield one or two significant accuracy in mostly scattering medium (Ω_0>0.7). Recalling Eqs. (16) and (17), for mostly absorbing medium ($\Omega_0 \rightarrow 0$), the integral equation is weakly coupled with the incident energy function $G(\tau)$. In fact, to obtain the incident energy and the net heat flux for pure absorbing (Ω_0=0) medium, Equation (16) is no longer an integral equation; it contains the analytical solution in the integral form. Therefore, as $\Omega_0 \rightarrow 1$, the integral equations become strongly coupled, and the accuracy of synthetic kernels, or; in other words, the influence of the goodness and order of the synthetic kernels relatively effects the SK_N solutions.

Table 2. The SK_N and the exact solutions of ρ and Γ for BMP-1 and for various optical dimensions and Ω_0, a_1 values.

		$a_1 = -1$		$a_1 = 0$		$a_1 = 1$	
Ω_0	**Case A**	ρ	Γ	ρ	Γ	ρ	Γ
	Exact	0.14581	0.31730	0.14108	0.32366	0.13626	0.33021
0.1	SK_1	0.14564	0.31732	0.14094	0.32372	0.13614	0.33029
	SK_2	0.14581	0.31740	0.14112	0.32376	0.13633	0.33025
	Exact	0.23316	0.35233	0.22045	0.37226	0.20695	0.39389
0.3	SK_1	0.23144	0.35259	0.21890	0.37280	0.20560	0.39454
	SK_2	0.23333	0.35358	0.22090	0.37340	0.20782	0.39446
	Exact	0.34088	0.40445	0.32261	0.43931	0.30240	0.47889
0.5	SK_1	0.33512	0.40530	0.31736	0.44077	0.29788	0.48041
	SK_2	0.34184	0.40930	0.32454	0.44363	0.30584	0.48124
	Exact	0.48132	0.48557	0.46060	0.53669	0.43676	0.59687
0.7	SK_1	0.46711	0.48734	0.44757	0.53911	0.42550	0.59824
	SK_2	0.48501	0.49972	0.46689	0.54898	0.44683	0.60394
	Exact	0.68002	0.62157	0.66044	0.68867	0.63694	0.76975
0.9	SK_1	0.64867	0.62378	0.63137	0.69036	0.61132	0.76791
	SK_2	0.69299	0.65994	0.67912	0.72087	0.66367	0.78903
	Case B						
	Exact	0.06660	0.04177	0.05996	0.04412	0.05313	0.04664
0.1	SK_1	0.06649	0.04180	0.05983	0.04414	0.05299	0.04661
	SK_2	0.06659	0.04179	0.05995	0.04414	0.05312	0.04665
	Exact	0.14853	0.05179	0.13016	0.06036	0.11012	0.07081
0.3	SK_1	0.14738	0.05225	0.12882	0.06071	0.10870	0.07060
	SK_2	0.14843	0.05211	0.13006	0.06069	0.11005	0.07097
	Exact	0.25325	0.07240	0.22620	0.09109	0.19503	0.11633
0.5	SK_1	0.24932	0.07458	0.22179	0.09302	0.19034	0.11660
	SK_2	0.25299	0.07397	0.22600	0.09263	0.19496	0.11708
	Exact	0.40193	0.12293	0.37216	0.16063	0.33620	0.21460
0.7	SK_1	0.39234	0.13160	0.36163	0.16922	0.32511	0.22011
	SK_2	0.40165	0.12946	0.37216	0.16674	0.33679	0.21778
	Exact	0.66813	0.30197	0.64996	0.37814	0.62749	0.48426
0.9	SK_1	0.65012	0.34430	0.63115	0.42233	0.60835	0.52514
	SK_2	0.67029	0.33749	0.65371	0.40910	0.63396	0.50178
	Case C						
	Exact	0.05234	0.26751	0.04566	0.27349	0.03881	0.27968
0.1	SK_1	0.05221	0.26745	0.04552	0.27349	0.03867	0.27968
	SK_2	0.05223	0.26752	0.04566	0.27351	0.03881	0.27969
	Exact	0.12660	0.29254	0.10750	0.31131	0.08686	0.33197
0.3	SK_1	0.12516	0.29190	0.10597	0.31095	0.08534	0.33174
	SK_2	0.12657	0.29274	0.10749	0.31149	0.08690	0.33210
	Exact	0.21789	0.33094	0.18786	0.36399	0.15365	0.40250
0.5	SK_1	0.21277	0.32855	0.18248	0.36228	0.14827	0.40107
	SK_2	0.21788	0.33171	0.18796	0.36470	0.15394	0.40305
	Exact	0.33704	0.39225	0.29797	0.44162	0.25097	0.50205
0.7	SK_1	0.32355	0.38535	0.28387	0.43580	0.23679	0.49648
	SK_2	0.33740	0.39451	0.29867	0.44375	0.25223	0.50384
	Exact	0.50720	0.49791	0.46120	0.56562	0.40270	0.65209
0.9	SK_1	0.47465	0.47892	0.42731	0.54787	0.36832	0.63405
	SK_2	0.50925	0.50407	0.46416	0.57155	0.40709	0.65736

Inhomogeneous Medium

For linearly and quadratically varying scattering albedos in isotropic, forward and backward anisotropic scattering medium, the exact RITE and the SK_N solutions of the hemispherical reflectivity and transmissivity values of the outer shell boundary of Cases A, B and C are tabulated in Table 3. For Case A, the reflectivity and transmissivity values obtained with SK_2 approximation yield two to three significant digit accuracies (absolute errors of less than 0.6%). In general, the SK_2 solutions show better performance than SK_1 approximation. On the other hand, absolute errors of reflectivity and transmissivity values using SK_2 approximation are less than 0.38% and 0.082% for Case B and C, respectively. These errors from the SK_N approximation are also influenced by the inner boundary condition and the accuracy of the synthetic kernels used.

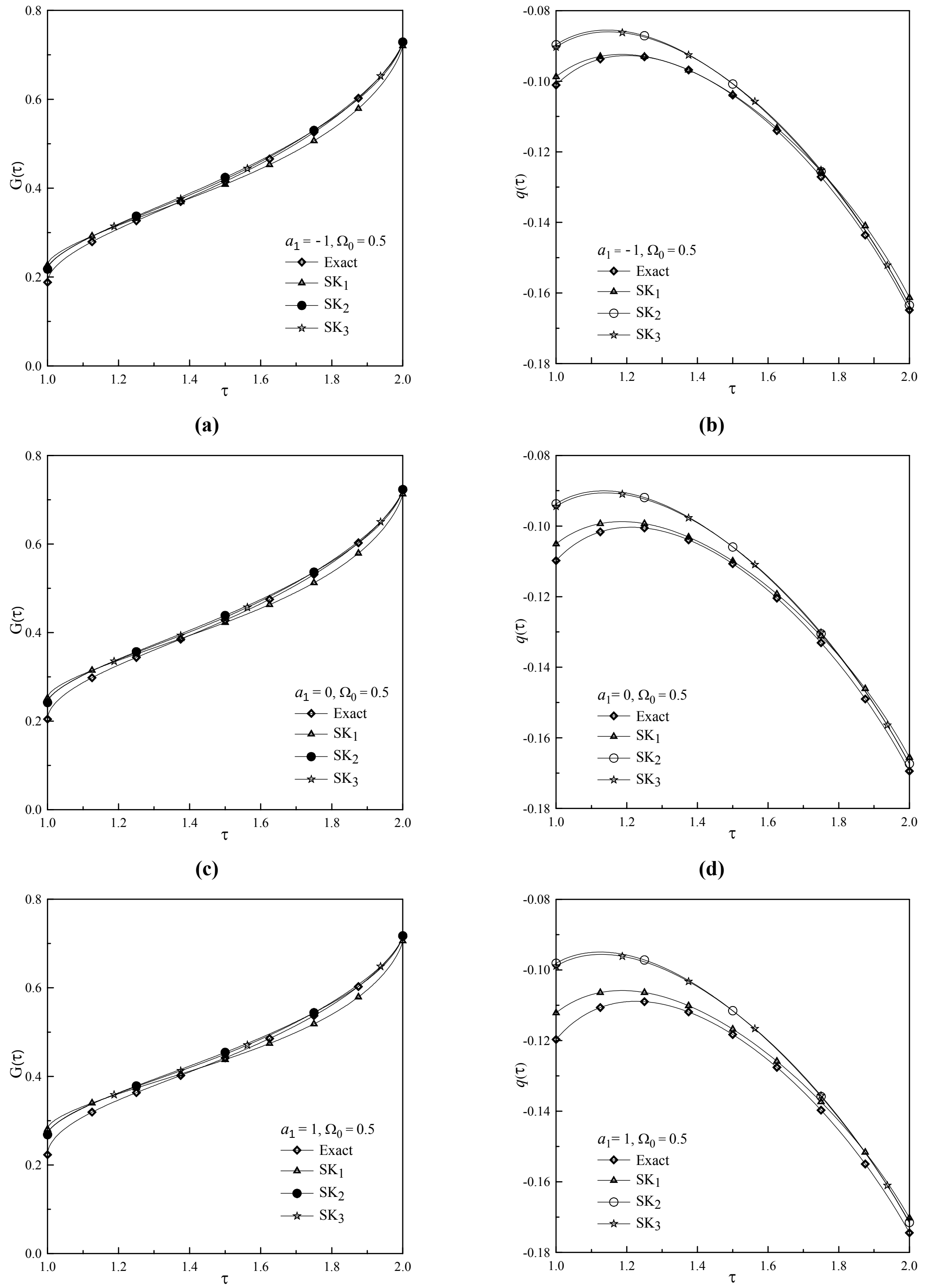

(f)

Figure 2. Profiles of the incident radiation and net radiative heat flux for Case A of forward anisotropic (a, b), isotropic (c, d), and backward anisotropic (e, f) scattering media (Ω_0=0.5).

The exact RITE and the SK_N solutions of the net radiative heat flux for Case B and C and $\Omega_0(\tau)=0.25+\tau/3F_1$ for isotropic, forward and backward scattering are depicted in Figure 4. This space-dependent scattering albedo choice represents an increase from 0.25 at the inner shell to 0.58 at the outer shell; that is scattering is higher at near the inner shell. The agreement between the exact and the SK_N solutions are excellent for $N\geq2$. However, in Case B, we observe sight deviations (Fig. 4(b) and (c)) near the inner shell. The magnitude of the difference from the exact values is small affecting only the second significant digits. In Figure 5, the exact RITE and the SK_N solutions of the net radiative heat flux for Case B and C and $\Omega_0(\tau)=0.75-\tau/3F_1$ for isotropic, forward and backward scattering medium are presented. The scattering albedo at the outer shell is 0.667 and declines to 0.42 at the inner surface. Therefore, the effect of the scattering albedo gradient within the medium on the SK_N approximation is sought. The net radiative heat flux profiles of the exact and the SK_N solutions are in good agreement. In Case B, the deviations near the inner shell are also observed here (Fig. 5(b) and (c)). The nature of this deviation is discussed in the next section.

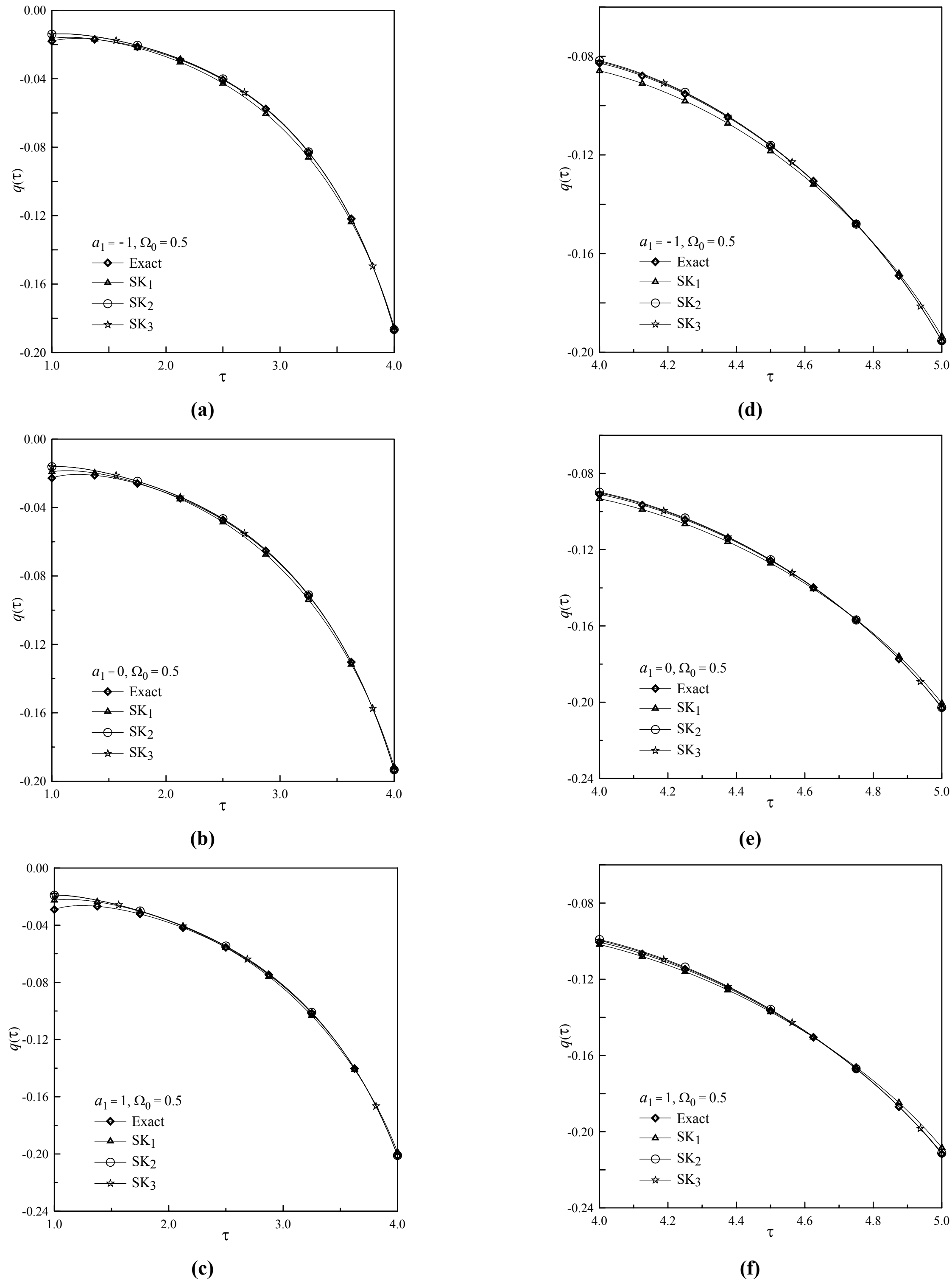

Figure 3. Profiles of the net radiative heat flux for Case B and C of forward anisotropic (a, d), isotropic (b, e), and backward anisotropic (c, f) scattering media (Ω_0=0.5).

Table 3. The SK_N The SK_N and the exact solutions of ρ and Γ for BMP-2 and for various optical dimensions and Ω_0, a_1 values.

$\Omega_0(\tau)$		$a_1=-1$		$a_1=0$		$a_1=1$	
Case A		ρ	Γ	ρ	Γ	ρ	Γ
$0.25+\tau/3F_1$	Exact	0.35331	0.39883	0.33406	0.43226	0.31278	0.47008
	SK_1	0.34621	0.39912	0.32739	0.43315	0.30674	0.47113
	SK_2	0.35389	0.40279	0.33555	0.43575	0.31567	0.47118
$0.75-\tau/3F_1$	Exact	0.32901	0.41074	0.31174	0.44698	0.29263	0.48828
	SK_1	0.32434	0.41201	0.30767	0.44884	0.28940	0.49005
	SK_2	0.33032	0.41661	0.31411	0.45225	0.29663	0.49125
$0.4-4\tau/15F_1+\tau^2/2F_2$	Exact	0.35971	0.39679	0.33993	0.42970	0.31808	0.46690
	SK_1	0.35190	0.39688	0.33253	0.43041	0.31126	0.46781
	SK_2	0.36006	0.40040	0.34116	0.43290	0.32067	0.46851
$1-16\tau/15F_1+\tau^2/2F_2$	Exact	0.33016	0.41073	0.31274	0.44707	0.29348	0.48848
	SK_1	0.32545	0.41210	0.32739	0.43315	0.29022	0.49034
	SK_2	0.33140	0.41663	0.31505	0.45236	0.29742	0.49145
Case B							
$0.25+\tau/3F_1$	Exact	0.28402	0.06605	0.25422	0.08196	0.21950	0.10310
	SK_1	0.27802	0.06724	0.24765	0.08295	0.21267	0.10280
	SK_2	0.28360	0.06688	0.25385	0.08274	0.21927	0.10340
$0.75-\tau/3F_1$	Exact	0.22463	0.08144	0.20049	0.10332	0.17295	0.13320
	SK_1	0.22231	0.08511	0.19771	0.10670	0.16995	0.13458
	SK_2	0.22451	0.08428	0.20043	0.10611	0.17305	0.13472
$0.4-4\tau/15F_1+\tau^2/2F_2$	Exact	0.29873	0.06560	0.26751	0.08134	0.23104	0.10222
	SK_1	0.29142	0.06666	0.25960	0.08212	0.22286	0.10160
	SK_2	0.29816	0.06646	0.26700	0.08217	0.23068	0.10258
$1-16\tau/15F_1+\tau^2/2F_2$	Exact	0.22621	0.08492	0.20175	0.10794	0.17390	0.13949
	SK_1	0.22370	0.08910	0.19878	0.11170	0.17070	0.14088
	SK_2	0.22605	0.08851	0.20166	0.11150	0.17401	0.14155
Case C							
$0.25+\tau/3F_1$	Exact	0.22323	0.33038	0.19255	0.36327	0.15759	0.40156
	SK_1	0.21769	0.32799	0.18674	0.36155	0.15179	0.40012
	SK_2	0.22316	0.33112	0.19258	0.36394	0.15781	0.40207
$0.75-\tau/3F_1$	Exact	0.21262	0.33154	0.18325	0.36476	0.14979	0.40348
	SK_1	0.20789	0.32914	0.17826	0.36304	0.14481	0.40204
	SK_2	0.21269	0.33236	0.18342	0.36551	0.15015	0.40407
$0.4-4\tau/15F_1+\tau^2/2F_2$	Exact	0.22650	0.33008	0.19542	0.36288	0.16000	0.40105
	SK_1	0.22069	0.32468	0.18934	0.36115	0.15393	0.39960
	SK_2	0.22637	0.33079	0.19540	0.36352	0.16017	0.40153
$1-16\tau/15F_1+\tau^2/2F_2$	Exact	0.21368	0.33143	0.18417	0.36463	0.15056	0.40332
	SK_1	0.20888	0.32903	0.17911	0.36292	0.14551	0.40189
	SK_2	0.21373	0.33224	0.18433	0.36537	0.15090	0.40390

On The Accuracy of SK_N Approximation

The SK_N equations, Eq. (24), and the boundary condition, Eq. (26), which are derived in this study are mathematically accurate and complete for homogeneous solid spherical geometry only. The SK_N formulation is also correct in cases where the extinction coefficient is constant, and the scattering coefficient, as in BMP-2, are functions of space. The causes of the errors in the SK_N approximation for homogeneous and inhomogeneous medium of described nature were covered in detail in Altaç, (2002a) and Altaç, (2002b) so we will not reiterate these arguments which are also valid for this study. But it should be pointed out that the magnitude of this type of errors are reduced by simply increasing the order of the approximation or using more accurate quadrature sets over the solution domain (Altaç, 2002a; Altaç, 2002b).

The SK_N formulation is not exact for inhomogeneous medium where the extinction coefficient is a function of space since optical path is defined as $\tau=\int_0^{|\mathbf{r}-\mathbf{r}'|}\beta(x)dx$. In this case, extra terms appear in the SK_N equations as well as in its boundary conditions. When the SK_N equations for inhomogeneous medium are written in the

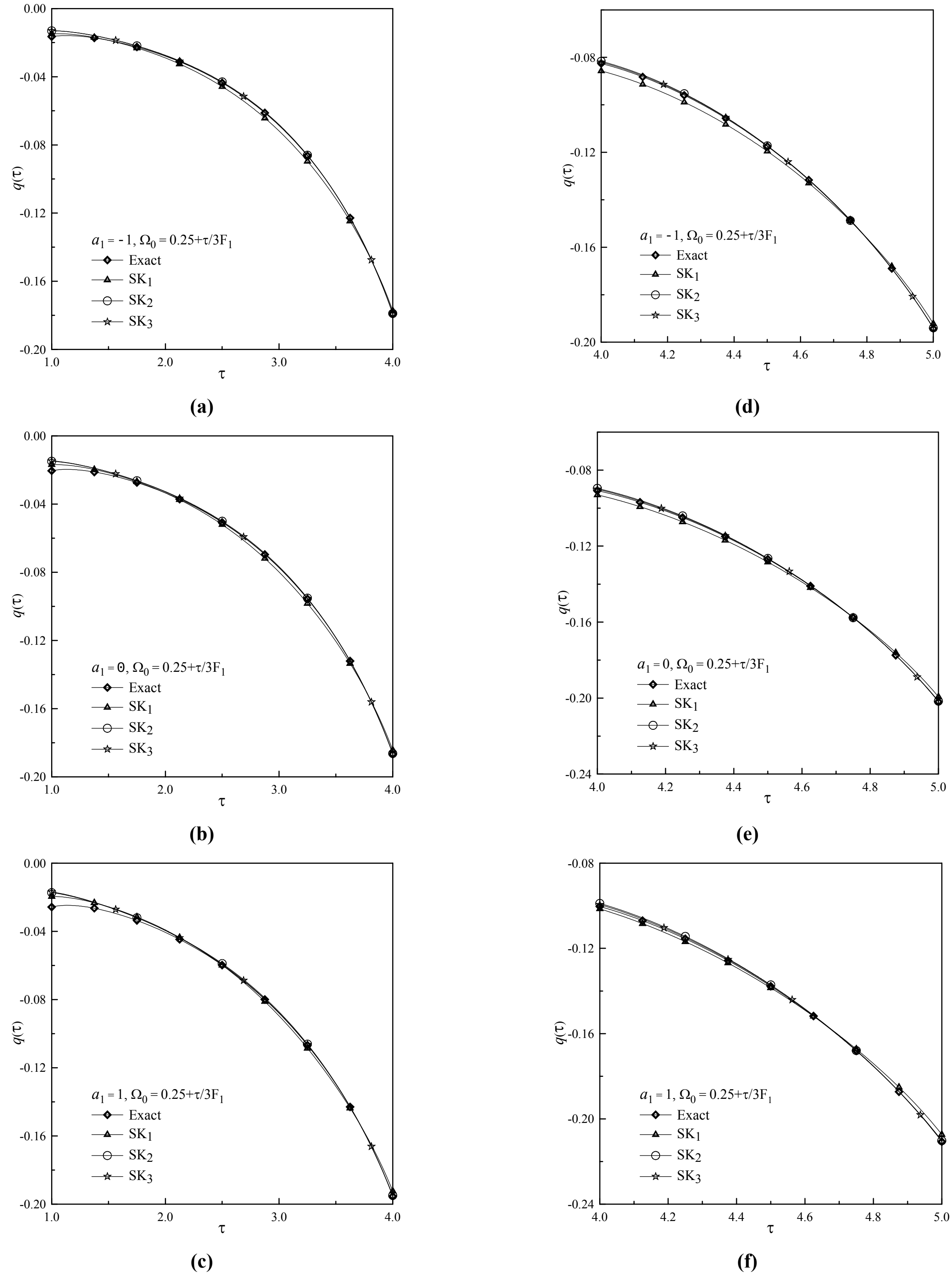

Figure 4. Profiles of the net radiative heat flux for spherical shell of radii τ_1=1.0 τ_2=4.0and, τ_1=4.0 τ_2=5.0, forward anisotropic (a, d), isotropic (b, e), and backward anisotropic (c, f) scattering in inhomogenous media ($\Omega_0(\tau)$=0.25+$\tau/3F_1$).

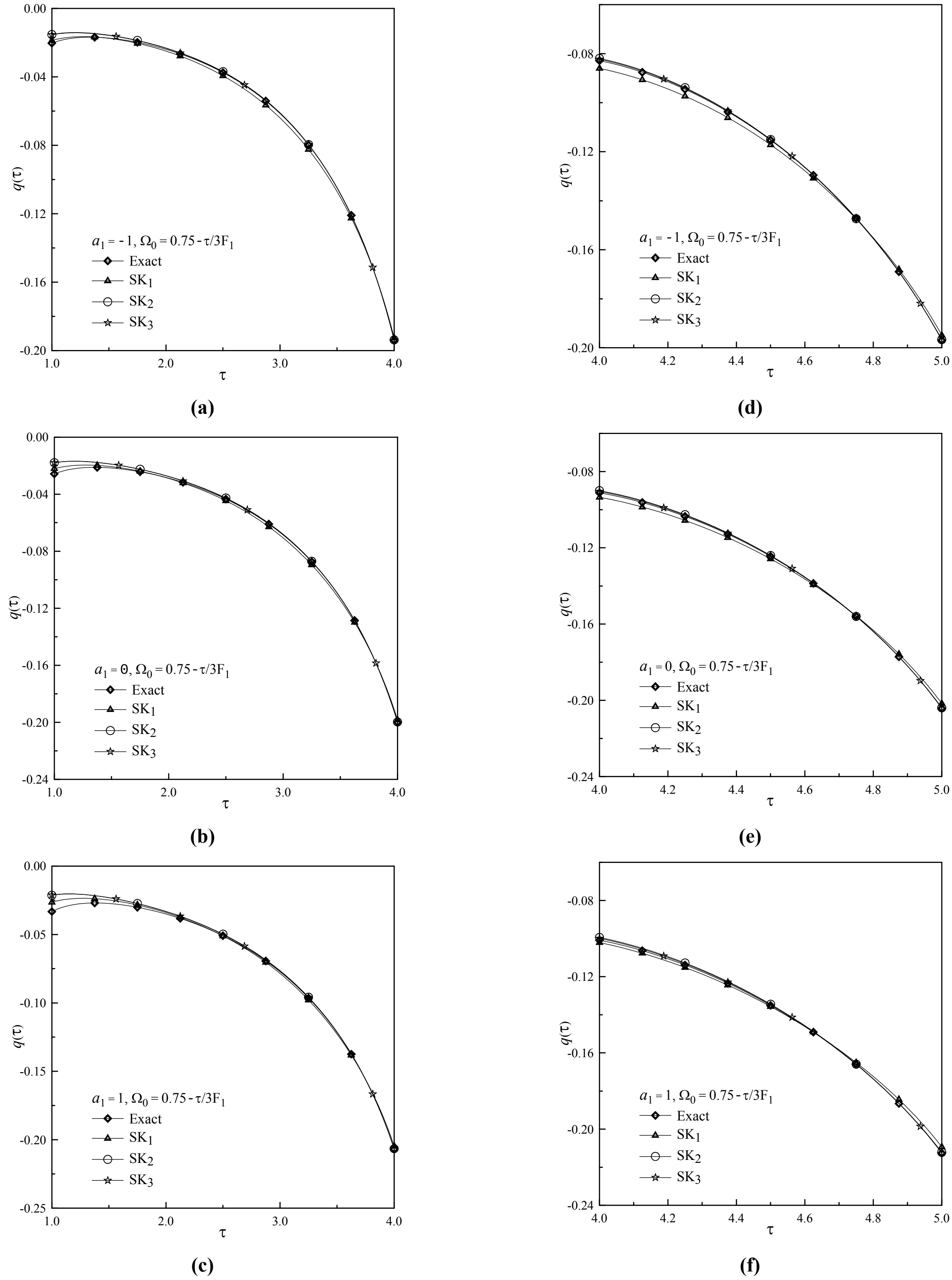

Figure 5. Profiles of the net radiative heat flux for spherical shell of radii τ_1=1.0 τ_2=4.0 and, τ_1=4.0 τ_2=5.0, forward anisotropic (a, d), isotropic (b, e), and backward anisotropic (c, f) scattering in inhomogenous media ($\Omega_0(\tau)$=0.75-$\tau/3F_1$).

dimensioned form, the coefficient of the Laplacian takes $-\nabla \cdot D_n(\mathbf{r})\nabla G_n$ form where $D_n(\mathbf{r}) = \mu_n^2 / \beta(\mathbf{r})$ (Spinrad and Altaç, 1990). However, it was shown that the SK_N method, remarkably, yields very good results even if the medium had a step-wise varying extinction coefficient (Altaç, 2002b). Similarly, when the SK_N equations are specifically derived for hollow spherical medium using Eqs. (16) and (17), extra terms which are in the integral forms appear in Eq. (20) and Eqs. (24—27). This yields complicated boundary conditions and thus numerical solution becomes more involved. To preserve the simplicity of the SK_N equations and the boundary conditions for the hollow sphere, these extra terms are "deliberately" neglected. And so this question arises, "why do we still get very good results by neglecting these extra terms?". To answer the question, we need to look at the general forms of the extra terms, which contain exponentials in the form of $\exp(-x/\mu_n)$ as in the approximate kernels—Eqs. (12)-(15). Noting that the Gauss quadrature abscissas for (0,1) interval are less than unity (μ_n<1), provided that x>0, as the order of approximation is increased the exponential terms decay very quickly ($\exp(-x/\mu_n)\to 0$). The extra terms for most of the synthetic components will approach zero except for the components corresponding $\mu_n \approx 1$. However, the weight of the largest abscissa of the Gauss quadratures is also the smallest which in turn the errors of this component are reduced; for example, the SK_3 quadrature μ_n =(0.1127, 0.5, 0.8873) and w_n= (0.2777, 0.4444, 0.2777). Therefore, the deviations or fluctuations in the extinction coefficient or extra terms do not significantly affect the solution.

One other approximation, which was introduced in this study, involves the derivation of the inner boundary condition. Equation (25) is obtained by neglecting the exponential terms in Eqs. (12-15) that contain $\lambda(\tau_1,\tau')$. This approximation will be valid if τ_1 and τ_2 are sufficiently large. The deviations that we observe in Case A and B of BMP-1 and 2 are mainly due to the inner shell boundary condition. For a larger inner shell radius and/or larger optical radius, $\tau_2-\tau_1$, the incident energy and heat flux profiles improve, as in Case B and C, impliying the decaying exponetial terms ($\exp(-\lambda(\tau_1,\tau')/\mu_n)\to 0$). For that reason, in homogeneous and/or inhomogeneous problems of Case C, we do not observe the deviations near inner shell. It is possible, however, to improve the inner shell boundary condition further by including the extra terms into the boundary conditions which will surely increase the cpu time.

CONCLUSION

The SK_N method was applied for the solution of thermal radiative transfer problems in hollow spherical participating homogeneous/inhomogeneous medium. The hemispherical reflectivity and transmissivity values for the outer shell boundary were computed with the SK_N method and the exact RITE. Quantitative comparison of solutions reveal that as the scattering albedo of the medium increases, solutions of one or two significant digit accuracy (absolute errors of less than 1.5%) are obtained. For absorbing medium, three to four significant digit accuracies (absolute errors of less than 0.5%) are common. A qualitative comparison of the incident energy and the net radiative heat flux solutions within the computational domain was also analyzed. Highly accurate solutions for optically thin systems and/or absorbing dominated medium can be obtained at very low order approximations. The heat flux and incident energy profiles of small inner shell radius geometries results in deviations near the inner boundary which is due to the approximation made for the inner boundary condition. This approximation yields better results for large inner shell radius (such as Case C) and/or larger optical thickness (such as Case B).

REFERENCES

Abramowitz M., Stegun, I.A., *Handbook of mathematical functions*, Dover Publications, 1964.

Altaç Z. and Spinrad B.I., The SK_N method I: A high order transport approximation to neutron transport problems, *Nucl. Sci. Eng.* 106, 471-479, 1990.

Altaç Z., The SK_N approximation for solving radiation transport problems in absorbing, emitting and scattering media, *Turkish J Eng. Env. Sci*. 21, 51-58, 1997.

Altaç Z. and Tekkalmaz M., The SK_N approximation for solving radiation transport problems in absorbing, emitting, and scattering rectangular geometries, *J Quant Spectrosc Radiat Transfer* 73, 219-230, 2002.

Altaç Z., The SK_N approximation for solving radiative transfer problems in absorbing, emitting, and isotropically scattering plane-parallel medium: Part 1, *J. Heat Transfer* 124, 674-684, 2002a.

Altaç Z., The SK_N approximation for solving radiative transfer problems in absorbing, emitting, and linearly anisotropically scattering plane-parallel medium: Part 2, *J Heat Transfer* 124, 685-695, 2002b.

Altaç Z. and Tekkalmaz M., The Synthetic Kernel (SK_N) Method applied to thermal radiative transfer in absorbing emitting, and isotropically scattering homogeneous and inhomogeneous solid spherical medium, *J Heat Transfer* 125, 739-746, 2003.

Altaç Z. and Tekkalmaz M., Radiative transfer in rectangular absorbing, emitting and isotropically scattering homogeneous medium using exact, discrete ordinate and synthetic kernel methods, *On Radiative Transfer in Participating Medium* (Eurotherm Seminar No. 73), April 14-17, Mons, Belgium, 11-22, 2003.

Altaç Z., Radiative transfer in absorbing, emitting and linearly anisotropic-scattering inhomogeneous cylindrical medium, *J Quant Spectrosc Radiat Transfer* 77, 172-192, 2003.

Altaç Z. and Tekkalmaz, M., Radiative transfer in one-dimensional hollow sphere with anisotropic scattering and variable medium properties, *J Quant. Spectrosc. Radiat. Transfer* 83/1, 115-117, 2004.

Crosbie A.L. and Khalil H.K., Radiative transfer in a gray isothermal spherical layer, *J Quant Spectrosc Radiat Transfer* 12, 1465-1486, 1972.

Döner N. and Altaç Z., Solution of the radiative transfer equation using the Synthetic Kernel (SK_N) method in inhomogeneous participating and anisotropically scattering one-dimensional cylindrical medium, *The Second International Conference On Thermal Engineering and Applications*, Al Ain, UAE , 176-180, 2006a.

Döner N. and Altaç Z., Solution of the radiative transfer equation using the Synthetic Kernel (SK_N) method in participating and anisotropically scattering one-dimensional medium, *Computational Radiative Transfer In Participating Media II* (Eurotherm Seminar 78), Poitiers, France, 1-10, 2006b.

Döner N. and Altaç Z., Solution of the radiative transfer problems in two-dimensional participating cylindrical medium with isotropic scattering using the SK_N approximation, *9th International Conference On Advanced Computational Methods And Experimental Measurements In Heat And Mass Transfer*, New Forest, United Kingdom, 109-120, 2006c.

El-Wakil S.A., Haggag M.H., Attia M.T. and Saad E.A., Radiative transfer in an inhomogeneous sphere, *J Quant Spectrosc Radiative Transfer* 40, 71-78, 1988.

El-Wakil S. A., Attia M.T. and Abulwafa E. M., Radiative transfer in a spherical inhomogeneous medium with anisotropic scattering, *J Quant Spectrosc Radiat Transfer* 46, 31-40, 1991.

Jia G., Yener Y. and Cipolla J. W., Radiation between two concentric spheres seperated by a participating medium, *J Quant. Spectrosc. and Radiat. Transfer* 46, 11-19, 1991.

Lee C. E., The discrete S_N approximation to transport theory, *Technical Information Series Report* LA2595, Lawrence Livermore Laboratory, 1962.

Lewis E.E. and Miller WF., *Computational methods of neutron transport*, John Wiley and Sons, 1984.

Li W. and Tong T.W, Radiative heat transfer in isothermal spherical media, *J Quant. Spectrosc. Radiat. Transfer* 43, 239-251, 1990.

Olfe D. B., Application of a modified differential approximation to Radiative transfer in a gray medium between concentric spheres and cylinders , *J Quant Spectrosc Radiat Transfer* 8, 899-907, 1968.

Ryhming I. L., Radiative transfer between two concentric spheres separated by an absorbing and emitting gas, *Int. J Heat Mass Transfer* 9, 315-324, 1966.

Thynell S.T. and Özişik M.N., Radiation Transfer in an isotropically scattering solid sphere with space dependent albedo, *J Heat Transfer* 107, 732-734, 1985a.

Thynell S.T. and Özışık M. N., Radiation transfer in an isotropically scattering homogenous solid sphere, *J Quant Spectrosc Radiat Transfer* 33, 319-330, 1985b.

Thynell S.T. and Özışık M.N., Radiation transfer due to a point source in anisotropically inhomogenous solid sphere, *J Quant Spectrosc Radiat Transfer* 35, 349-356, 1986.

Thynell S.T., Radiative transfer in absorbing, emitting and linearly anistropically scattering pherical media, *J Quant Spectrosc Radiat Transfer* 41, 383-395, 1989.

Tong T.W. and Swathit P.S., Radiative Heat Transfer in Emitting-Absorbing-Scattering Spherical Media, *J Thermophysics Heat Transfer* 1, 162-170, 1987.

Trabelsi H., Sghaier T. and Sifaoui M.S., A theoretical study of radiation between two concentric spheres using a modified discrete ordinates method associated with Legendre transform, *J Quant. Spectrosc. Radiat. Transfer* 93, 415-428, 2005.

Traugott S.C., An improved differential approximation for radiative transfer with spherical symmetry, *AIAA Journal* 7, 1825-1832, 1969.

Tsai J. R., Özışık M. N. and Santarelli R., Radiation in spherical symmetry with anisotropic scattering and variable properties, *J Quant Spectrosc Radiat Transfer* 42, 187-199, 1989.

Sghaier T., Sifaoui M.S. and Soufiani A., Study of radiation in spherical media using discrete ordinates method associated with the finite Legendre transform, *J Quant Spectrosc Radiat Transfer* 64, 339-351, 2000.

Spinrad B.I. and Altaç Z. The SK_N method II: Heterogeneous problems, *Nucl. Sci. Eng*. 106, 480-488, 1990.

Viskanta R. and Crosbie A. L., Radiative transfer through a spherical shell of an absorbing-emitting gray medium, *J Quant Spectrosc Radiat Transfer* 7, 871-889, 1967.

Wilson S.J. and Nanda T.R., Radiative transfer in absorbing, emitting and linearly anisotropically scattering inhomogeneous solid spheres, *J Quant Spectrosc Radiat Transfer* 44, 345-350, 1990.

Mesut TEKKALMAZ, 1972 Eskişehir doğumludur. İlk, orta ve lise öğrenimini Eskişehir'de tamamladı. 1994 yılında Anadolu Üniversitesi Mühendislik ve Mimarlık Fakültesi Makina Mühendisliğinden mezun oldu. 1995 yılında Eskişehir Osmangazi Üniversitesi Mühendislik ve Mimarlık Fakültesi Makina Mühendisliği Bölümünde araştırma görevlisi oldu. Eskişehir Osmangazi Üniversitesi Fen Bilimleri Enstitüsü, Makina Mühendisliği Anabilim dalında 1996 yılında yüksek lisans ve 2003 yılında doktora öğrenimini tamamladı. Halen Eskişehir Osmangazi Üniversitesi Mühendislik ve Mimarlık Fakültesi Metalurji ve Malzeme Mühendisliği Bölümünde görev yapmaktadır. Evli ve bir çocukludur.

Zekeriya ALTAÇ, 1962 Siirt doğumludur. İlk ve orta öğrenimini Siirt'te, Lise öğrenimini Eskişehir'de tamamladı. İTÜ Kimya-Metalurji Fakültesi Metalurji Mühendisliği Bölümü mezunudur. MEB burslu olarak ABD'de Iowa State Üniversitesi Nükleer Enerji Mühendisliği Bölümünde Yüksek Lisans ve Doktorasını tamamlayarak, 1989 yılında Anadolu Üniversitesi MMF Makine Mühendisliği Bölümünde göreve başladı. 1992 yılında Doçent, 1998 yılında Profesör ünvanını aldı. Halen Eskişehir Osmangazi Üniversitesi Mühendislik ve Mimarlık Fakültesi Makina Mühendisliği Bölümünde görev yapmaktadır. Evli ve bir çocukludur.